ACS APPLIED MATERIALS & INTERFACES

Research Article

Cite This: ACS Appl. Mater. Interfaces 2020, 12, 2601−2606

www.acsami.org

Ten-Input Cube Root Logic Computation with Rational Designed DNA Nanoswitches Coupled with DNA Strand Displacement Process

Chunyang Zhou,*[,†,‡] Hongmei Geng,[†] Pengfei Wang,*[,‡] and Chunlei Guo*[,†,§]

[†]The Photonics Laboratory, Changchun Institute of Optics, Fine Mechanics and Physics, Chinese Academy of Sciences, Changchun, Jilin 130033, China

[‡]Institute of Molecular Medicine, State Key Laboratory of Oncogenes and Related Genes, Renji Hospital, School of Medicine, Shanghai Jiao Tong University, Shanghai 200127, China

[§]The Institute of Optics, University of Rochester, Rochester, New York 14627, United States

Supporting Information

ABSTRACT: The predictability of Watson−Crick base-pairing provides a unique structural programmability to DNAs, promoting a facile design of bimolecular reactions that perform computation. However, most of the current architectures could only implement limited logical circuits and are incapable of handling more complex mathematical operations, thus limiting computing devices from advancing to the next-stage functional complexity. Here, by designing a multifunctional DNA-based reaction platform coupled with multiple fluorescent substrates as output reporters, we construct, for the first time, a logic circuit that can compute the cube root of a 10-bit binary number (within the decimal number 1000). This relatively large-scale logic system with 10 inputs and four outputs showcases the power of DNAs in the field of biological computing and will potentially open up a new horizon for designing novel functional devices and complex computing circuits and bringing breakthroughs in biocomputing.

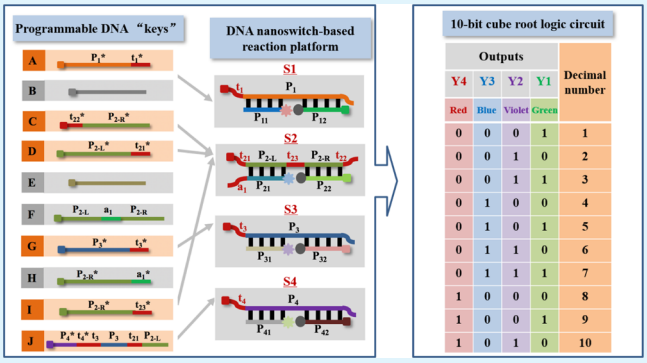

KEYWORDS: *DNA computing, cube root, large scale, toehold-mediated reaction, logic circuit*

INTRODUCTION

In order to develop the information chemistry as a programming technique that allows substances to function in ways that biological systems do not, it is necessary to understand how molecular interactions are coded and implemented. Relatively simple units that self-assemble into complex products are particularly suitable for this type of research.[1−3] The theory of combining the mathematical model with the statistical mechanical models of molecular crystallization shows that the algorithmic behavior can be embedded in the molecular self-assembly process, which has been demonstrated experimentally with Watson−Crick-based DNA nanotechnology.[4−7] Decision-making and other types of information processing may be realized in DNA nanodevices by using the concept of DNA computation, which exploits the inherent sequence programmability of DNA-based reactions. Importantly, the base-pairing specificity and sequence programmability of DNA provide unique design flexibility to such nanodevices, which have shown to be able to achieve from simple to complex biomolecular-based logic algorithm operations both in solution and on surfaces.[8−10] Such capabilities may be used in different fields such as drug release, switchable nanophotonics, or the construction of artificial biomolecular motors.[11] Although the pioneering work of Adleman and others was still devoted to address complex computational problems using biomolecular techniques, the focus of the field has shifted to the implementation of DNA-based logic circuits and dynamic reaction networks.[12]

Up to now, fluorescent, electrochemical, colorimetric, and other kinds of DNA logic devices/nanoswitches[13−21] are fabricated to realize various basic logic gates, advanced logic circuits and even neural networks, which fully prove the significance of biomolecular logic gates in biocomputing science.[22−24] However, most of them are still capable of realizing relative simple logic operations, the requirement for time-consuming procedures of conjugation with materials,[25,26] perishable protein enzymes,[27,28] and color-dependent read-out[29] impedes the development of biocomputing in the realization of more functional and complex logic circuits. Thus, the establishment of an enzyme-free DNA-based platform for constructing complex logic gates with sorting to precise analytical instrumentation is attractive and desperately needed. Qian and Winfree used a simple DNA reaction mechanism to demonstrate several digital logic circuits and

Received: September 2, 2019
Accepted: December 23, 2019
Published: December 23, 2019

DOI: 10.1021/acsami.9b15180
ACS Appl. Mater. Interfaces 2020, 12, 2601−2606

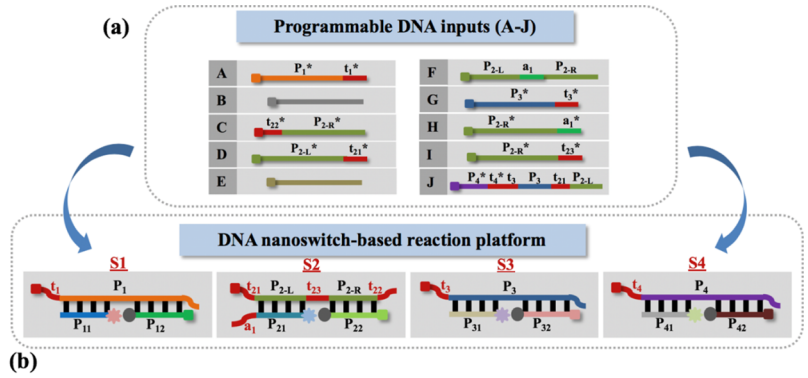

(b)

Cubic roots of integers	Inputs										Logic Processing	Outputs				Decimal number
	2^9	2^8	2^7	2^6	2^5	2^4	2^3	2^2	2^1	2^0		Y4	Y3	Y2	Y1	
	J	I	H	G	F	E	D	C	B	A		Red	Blue	Violet	Green	
1^3	0	0	0	0	0	0	0	0	0	1	S1 $(0<N\leq 2^3)$	0	0	0	1	1
2^3	0	0	0	0	0	0	1	0	0	0	S2 $(2^3\leq N\leq 3^3)$	0	0	1	0	2
3^3	0	0	0	0	0	1	1	0	1	1		0	0	1	1	3
4^3	0	0	0	1	0	0	0	0	0	0	S3 $(4^3\leq N\leq 7^3)$	0	1	0	0	4
5^3	0	0	0	1	1	1	1	1	0	1		0	1	0	1	5
6^3	0	0	1	1	0	1	1	0	0	0		0	1	1	0	6
7^3	0	1	0	1	0	1	0	1	1	1	S4 $(8^3\leq N\leq 10^3)$	0	1	1	1	7
8^3	1	0	0	0	0	0	0	0	0	0		1	0	0	0	8
9^3	1	0	1	1	0	1	1	0	0	1		1	0	0	1	9
10^3	1	1	1	1	1	0	1	0	0	0		1	0	1	0	10

Figure 1. Reaction mechanism of the DNA-based 10-bit cube root logic operation. (a) Description of the composition of input DNAs (A–J) and DNA-based nanoswitches (S1–S4). (b) Truth table of the 10-bit cube root logic operation.

finally constructed a four-bit square-root circuit that comprises 130 DNA strands.[11]

Recent advances in nanoscience have shown that DNA switches (rationally designed DNA nanostructures) are versatile building blocks for the fabrication and assembly of nanoscale computing devices and sensors.[30,31] Because structural switching molecules are reversible and endowed with significant affinity and specificity, they can work continuously in complex environments. This is well suited to numerous nanotechnology applications, and increasing efforts are being done to apply them to engineering applications.[32] Based on the above research, in this work, for the first time, by using DNA strand displacements, a 10-input and four-output cube root logic circuit has been successfully built to compute the 10-bit cube root logic circuit. In this 10-bit cube root logic operation, we aim to get a binary result that is equal to a decimal positive integer. The operation range in this work is to realize the cube root operation of the decimal number within 1000. In order to realize the 10-bit cube root logic circuit to calculate the cube root of the decimal number within 1000, a multifunctional platform that consists of a series of DNA-based nanoswitches is designed. Such DNA nanoswitches can be utilized as the reacting platform and allosterically regulated by specific DNA inputs to output the corresponding fluorescence signals in a controlled fashion by the toehold-mediated reaction (Figure 1). The four different fluorescent dyes have been modified on the four nanoswitches, and the signals of which can be regulated in a controlled manner. One of the keys of this work is that each of nanoswitches is programmed to have one or more recognition elements for its ability to specifically bind to a desired input stimulus, providing the appropriate conformational change for the specific output mechanism for the operation of 10-bit cube root logic circuit.

EXPERIMENTAL SECTION

Materials and Apparatus. All of the DNAs are listed in the Supporting Information (Table S1). All chemicals used in this work are of analytical reagent without purification. The concentrations of the DNA sequences are quantified by nanodrop. The fluorescence emission spectra were tested in Tris-HCl buffer in room temperature. The emission of the 6-carboxyfluorescein (FAM), 6-carboxyl-X-rhodamine (ROX), hexachlorofluorescein (HEX), and cyanine 5 (Cy5) are recorded at 517, 605, 556, and 665 nm.

Statistical Analysis. First, the concentrations of the DNA switches, including S1, S2, S3, and S4, have been optimized. The P_1, P_2, P_3, and P_4 were confirmed to be 150, 150, 125, and 150 nM as the optimized concentrations, respectively (Figure S3). Then, the P_{11}, P_{21}, P_{31}, and P_{41} are all optimized to be 125 nM. The P_{12}, P_{22}, P_{32}, and P_{42} are confirmed to be 200, 175, 225, and 175 nM as the optimized concentrations (Figure S2). The optimizations of the inputs were all confirmed to be 350 nM, respectively.

Logic Circuit Operation. According to our previous work,[33,34] all if the DNAs are annealed in 90 °C for 10 min before use. First of all, the DNA switches (S1, S2, S3 and S4) were synthesized and used as the platform to operate 10-4 cube root logic gate in this investigation. Then, the corresponding inputs were added into the nanoswitch-based platform for the logic operation according to the truth table.

RESULTS AND DISCUSSION

In this work, based on the DNA hybridization and TDSD, a multifunctional reaction platform with a series of DNA nanoswitches (S1, S2, S3, and S4) have been designed with multiple protruding toehold sites (Figure 1a). Taking the first nanoswitch of S1 as an example, which consists of the single-stranded P_1, P_{11}, and P_{12}, in which P_{11} is modified by FAM and

DOI: 10.1021/acsami.9b15180
ACS Appl. Mater. Interfaces 2020, 12, 2601−2606

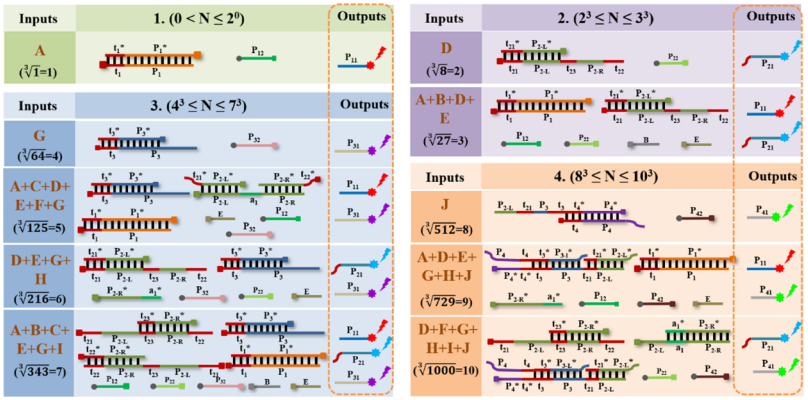

Figure 2. Hybridization reactions between the inputs and DNA nanoswitch-based platform for the realization of 10-bit cube root logic operation.

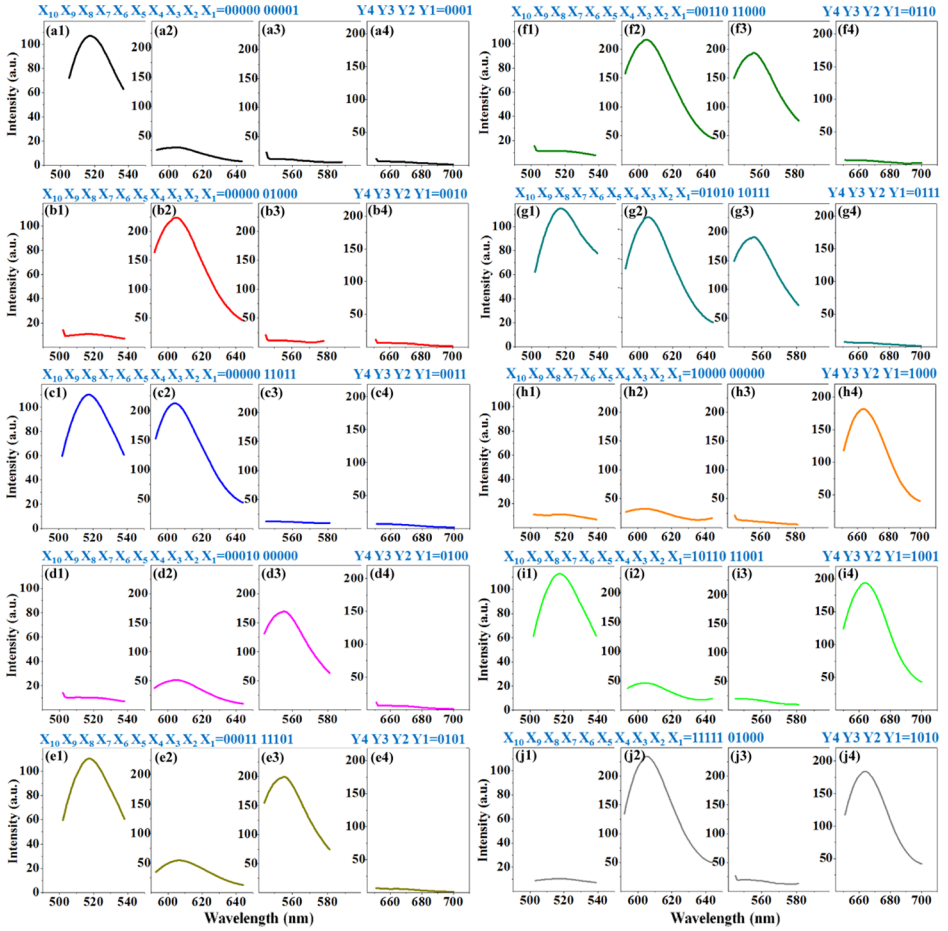

Figure 3. Fluorescence outputs (from the decimal number of 1−10) corresponding to different inputs ranging from 1 to 1000 in the 10-bit logic circuit. Panels from (a1) to (j1) showed the FAM fluorescence output of Y1. Panels from (a2) to (j2) showed the ROX fluorescence output of Y2. In (a3) to (j3), the HEX fluorescence intensity showed the output signal of Y3. In (a4) to (j4), the Cy5 fluorescence intensity showed the output signal of Y4.

P_{12} is modified by corresponding quencher (BHQ1, black hole quencher 1). In the initial state of S1, P_1 can hybridize with both P_{11} and P_{12} to form the duplex of $P_1/(P_{11} + P_{12})$ and shorten the distance between FAM and BHQ1. Therefore, the fluorescence resonance energy transfer (FRET) happens between them and leads to the decreased fluorescence of FAM. The second nanoswitch of S2 consists of single-stranded P_2 ($t_{21}P_{2\text{-}L}t_{23}P_{2\text{-}R}t_{22}$), P_{21}, and P_{22}, in which P_{21} is modified by the fluorescent dye of ROX and quenched by BHQ2 (black hole quencher 2) that modified on P_{22}. The S3 consists of P_3, P_{31}, and P_{32}, in which P_{31} is modified by the fluorescent dye of HEX and quenched by BHQ1 that modified on P_{32}. The S4 consists of P_4, P_{41}, and P_{42}, in which P_{41} is modified by the fluorescent dye of Cy5 and quenched by BHQ3 (black hole quencher 3) that modified on P_{42}. As shown in Figure S1, the designed four DNA nanoswitches can be turned on and lit up by specific input signals, performing different fluorescent output signals (FAM, ROX, HEX, and Cy5, which are defined as "red, blue, violet, and green" output signals). As shown in Figure 1, the inputs (A, B, C, D, E, F, G, H, T, J) are designed

DOI: 10.1021/acsami.9b15180
ACS Appl. Mater. Interfaces 2020, 12, 2601−2606

to specifically light one or more DNA nanoswitches by TDSD. As the exclusive "key" of S1, the input A ($P_1^*t_1^*$) can hybridize with S1 (t_1P_1) through the toehold site of t_1^*, releasing P_{11} and lengthening the distance between P_{11} and P_{12}, resulting in the enhanced fluorescence output signal of FAM (Figure S1, curve a1 and curve a2). The inputs C ($t_{22}^*P_{2\text{-R}}^*$), D ($P_{2\text{-L}}^*t_{21}^*$), and I ($P_{2\text{-R}}^*t_{23}^*$) are programmed to light up S2 through their specific toehold sites (t_{22}^*, t_{21}^*, and t_{23}^*) and eventually enhance the ROX fluorescence signal (Figure S1, curves c1 and c2, curves d1 and d2, curves i1 and i2). The input G ($P_3^*t_3^*$) is designed as the "key" of S3 (t_3P_3) to light up the fluorescence of HEX by the toehold site of t_3^* (Figure S1, curves g1 and g2). The input J ($P_4^*t_4^*$) is designed to light up the fluorescence of Cy5 by hybridizing with S4 (t_4P_4) (Figure S1, curves j1 and j2). As shown in the comparison curves of the state of "ON" and "OFF" (Figure S1), the fluorescence intensity of "OFF" state is low and performs a perfect low background signals, which can greatly improve the programmability and the accuracy of logic operation.

Before implementing the cube root logic operation, the optimum conditions for the formation of nanoswithches have been determined first (details in Figures S2 and S3). Furthermore, different concentrations of inputs are optimized to light up the DNA nanoswitch-based platform (details in Figure S4). As shown in Figure 1b, the possible values of variables as inputs and the corresponding function values as outputs are listed, which is the so-called truth table. The truth table represents logical functions in the form of a table, which has the advantage of being straightforward. Once the value of the input variable is determined, the corresponding function value can be found from the table. Therefore, it can plan in advance the logical relationship between the inputs and outputs of the logical operation to be implemented in binary language. For inputs, the absence of input is set as "0", otherwise, it is set as "1" for presence. For outputs, the corresponding high fluorescence intensity is defined as "1", otherwise, it is defined as "0". By encoding different combinations of inputs and adding them to the reaction platform made up of four DNA nanoswitches, the specific combination of output signals can be obtained (Y1−Y4, which is defined as four colors, red, blue, violet, and green). As the computational range increases, more and more DNA nanoswitches will be turned on, leading to an increase in the types of fluorescent output signals. Therefore, in this work, by dividing the calculation scope ($0 < N \leq 2^0$, $2^3 \leq N \leq 3^3$, $4^3 \leq N \leq 7^3$ and $8^3 \leq N \leq 10^3$), the working mechanism of 10-bit cube root logic operation can be clarified more clearly, which provides an important reference to realize the larger-scale logic operation in the future.

Figure 2 shows the reaction mechanism to realize the 10-bit cube root logic circuit in different ranges of calculation ($0 < N \leq 2^0$, $2^3 \leq N \leq 3^3$, $4^3 \leq N \leq 7^3$ and $8^3 \leq N \leq 10^3$), with the corresponding output fluorescence signals shown in Figure 3. The 10-bit cube root logic operation is start with the first calculation range ($0 < N \leq 2^0$). This calculation range includes only one case, namely, calculating the cube root of the decimal integer "1", in which the input strand of A should be added to the DNA nanoswitch-based platform. The input A ($P_1^*t_1^*$) can hybridize with t_1P_1 through the toehold site of t_1^* to recover the fluorescence of FAM that modified on P_{11} according to FRET (Figure 3a1), and other nanoswitches remained "off" with low fluorescence (Figure 3a2−a4). The enhanced fluorescent signal FAM (Y1) and the remaining inactive fluorescent signals (Y2, Y3, Y4) in the truth table have a binary code of "0001", which is the "1" in the decimal number. Therefore, the calculating result is that the cube root of "1" is equal to "1" ($\sqrt[3]{1} = 1$). In the second calculation range ($2^3 \leq N \leq 3^3$), there are two cases where the cube roots of the decimal integers "8" and "27" are calculated. For the calculation of the cube root of decimal "8", the input D ($P_{2\text{-L}}^*t_{21}^*$) should be added to the DNA nanoswitch-based platform and hybridize with nanoswitch S2 ($t_{21}P_{2\text{-L}}$) through the toehold site of t_{21}^*. Therefore, P_{21} modified by the fluorescence of ROX is released and performing a higher fluorescence signal (Figure 3b2), where the calculating result is that the cube root of decimal "8" is equal to decimal positive integer "2" ($\sqrt[3]{8} = 2$). To calculate the cube root of decimal "27", the input A ($P_1^*t_1^*$), B, D ($P_{2\text{-L}}^*t_{21}^*$), and E should be added to the platform. As mentioned above, the input A can hybridize with nanoswitch S1 (t_1P_1) and input D can hybridize with nanoswitch S2 ($t_{21}P_{2\text{-L}}$). Therefore, the fluorescences of FAM and ROX are lit up at the same time (Figure 3c1,c2), indicating the output signals of Y1 and Y2 are defined as "1" with the result that the cube root of decimal "27" is equal to decimal positive integer "3" ($\sqrt[3]{27} = 3$). In this work, in order to save time and cost, inputs B and E can be coded as not participating in the reaction, which will provide more coding space for us to realize a larger range of logical calculation in the subsequent work.

When the calculating value is increased to the third range ($4^3 \leq N \leq 7^3$), there are four calculation cases, namely, calculating the cubic root of the decimal integer "64", "125", "216", and "343". First, to calculate the cube root of decimal "64", the input G ($P_3^*t_3^*$) should be added to the platform and hybridize with S3 (t_3P_3) through the toehold site of t_3^*, enhancing the fluorescence of HEX that modified on P_{31} (Figure 3d3) and showing the result that the cube root of "64" is "4" ($\sqrt[3]{64} = 4$). Second, to calculate the cube root of decimal "125", the inputs A, C, D, E, F, and G are needed to add to the platform. In this case, as mentioned above, the input A ($P_1^*t_1^*$) can light up S1 and induce the fluorescence enhancement of FAM and G ($P_3^*t_3^*$) can light up S3 and induce the fluorescence enhancement of ROX (Figure 3e1,e3), indicating the output signals of Y1 and Y3 are defined as "1". Furthermore, to inhibit the increasing of output Y2 (ROX) induced by the inputs C and D, input F is programmed to preferentially hybridize with C and D, shutting down their sequence sites to switch on the nanoswitches of S2 and inhibit the enhancement of fluorescence intensity of ROX (Figure 3e2). Therefore, the enhancements of Y1 and Y3 show the calculating result of the decimal "125" is equal to decimal positive integer "5" ($\sqrt[3]{125} = 5$). Third, to calculate the cube root of decimal number "216", inputs D, E, G, and H are programmed to be added to the platform. In this case, inputs D and G are involved in hybridization and light up the nanoswitches of S2 and S3, indicating that the output signals of Y2 and Y3 are defined as "1" with the mean that the cube root of decimal "216" is equal to decimal positive integer "6" ($\sqrt[3]{216} = 6$) (Figure 3f1−f4). Next, to figure out the cube root of decimal number "343", inputs A, B, C, E, G, and I should be added. In this case, the inputs C ($t_{22}^*P_{2\text{-R}}^*$) and I ($P_{2\text{-R}}^*t_{23}^*$) are programmed to light up S2 based on the toehold site of t_{22}^* and t_{23}^* to recover the fluorescence signal of ROX (Figure 3g2), showing the result of the cube root of "343" is "7" ($\sqrt[3]{343} = 7$).

DOI: 10.1021/acsami.9b15180
ACS Appl. Mater. Interfaces 2020, 12, 2601−2606

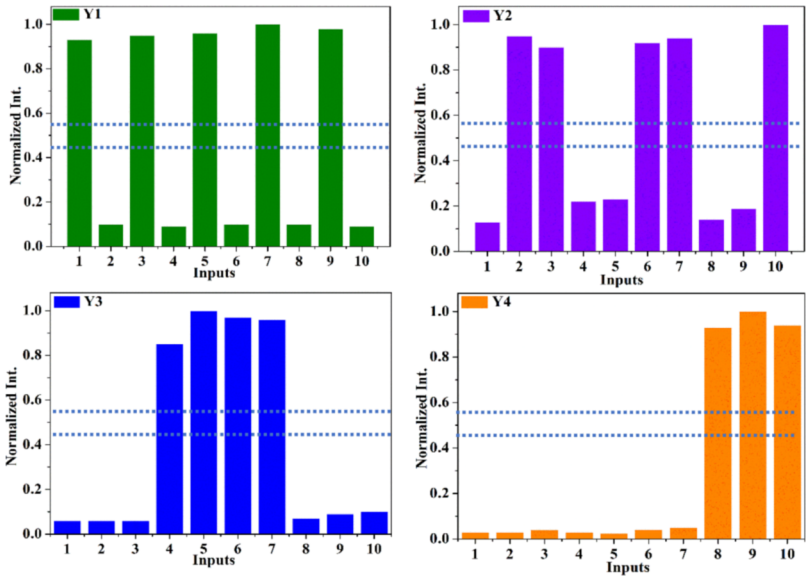

Figure 4. Histogram of the normalized fluorescence intensities of the four outputs (Y1, Y2, Y3, and Y4).

In the fourth calculation range ($8^3 \leq N \leq 10^3$), there are three cases where the cube roots of the decimal integers "512", "729", and "1000" are calculated. First of all, in order to figure out the cube root of decimal "512", the input J ($P_4^*t_4^*$) is programmed to be added to the platform and hybridize with t_4P_4 based on the toehold site of t_4^* (Figure 3h4), indicating the result of the cube root of decimal "512" is equal to the decimal positive integer "8" ($\sqrt[3]{512} = 8$). Second, to figure out the cube root of the decimal number "729", inputs A, D, E, G, H, and J are programmed to be added to the platform. In this case, input J (t_3P_3-$t_{21}P_{2\text{-}L}$) is also designed to hybridize with input D ($P_{2\text{-}L}^*t_{21}^*$) and input G ($P_3^*t_3^*$) to block their hybridization sites where they can switch on the nanoswitches of S2 and S3, inhibiting the enhancement of fluorescence intensity of ROX and HEX (Figure 3i2,i3). Therefore, the "turn-on" nanoswitches of S1 and S4 show the result of the cube root of "729" is "9" ($\sqrt[3]{729} = 9$). Finally, to figure out the cube root of decimal number "1000", inputs D, F, G, H, I, and J are programmed to be added to the platform. In this case, in order to inhibit the output signal of S3, input J (t_3P_3-$t_{21}P_{2\text{-}L}$) is also designed to hybridize with input D ($P_{2\text{-}L}^*t_{21}^*$) and input G ($P_3^*t_3^*$) to prevent the fluorescence intensity of ROX and HEX (Figure 3j3). Also, input F ($a_1P_{2\text{-}R}$) is designed to prefer to hybridize with input H ($P_{2\text{-}R}^*t_{23}^*$) based on the toehold site of a_1 to block the hybridization site to hybridize with input I, which can improve the fluorescence efficiency of S2. Therefore, the "turn-on" nanoswitches of S2 and S4 show the result of the cube root of decimal "1000" is equal to the decimal positive integer "10" ($\sqrt[3]{1000} = 10$).

As shown in Figure 4, the normalized outputs (Y1, Y2, Y3, and Y4) are plotted to define the threshold value. The output thresholds are defined as "1" when the normalized values are higher than 0.55, and otherwise, it can be defined as "0" when lower than 0.45. Thanks to the thresholding, the outputs can achieve ideal ON and OFF signals. In order to further identify the DNA hybridizations in the realization of the 10-bit cube root operation, the PAGE experiments are showed in Figure S5.

CONCLUSIONS

In conclusion, by designing a set of multifunctional DNA nanoswitches as reaction platform, a 10-bit cube root logic operation has been successfully constructed. It is the first time that a 10-bit cube root logic operation with 10 inputs and four outputs has been constructed on nanoswitch platform for the function of calculating the cube root within the decimal numbers of 1000. Significantly, in order to realize this relatively large-scale logic operation, the predictable base-pairing is used as the key role in this work, which offers such a powerful database and DNA structure programmability that opens up exciting prospects for designing functional devices and complex computational circuits.

ASSOCIATED CONTENT

Supporting Information

The Supporting Information is available free of charge at https://pubs.acs.org/doi/10.1021/acsami.9b15180.

All the sequences used in the experiment; working principle of the designed platform; optimal platform and inputs for the operation of cube root; and PAGE analysis of the interaction between DNA nanoswitch-based platform and inputs (PDF)

AUTHOR INFORMATION

Corresponding Authors

*E-mail: cyzhou@ciomp.ac.cn (C.Z.).
*E-mail: pengfei.wang@sjtu.edu.cn (P.W.).
*E-mail: guo@optics.rochester.edu (C.G.).

ORCID

Chunyang Zhou: 0000-0003-1165-5021
Pengfei Wang: 0000-0002-3125-763X
Chunlei Guo: 0000-0001-8525-6301

Author Contributions

C.Z. designed and performed the experiment, analyzed the data results, and prepared the formulation of the paper. H.G. participated the experiment and followed the progress of the project. C.G. and P.W. participated in the preparation of the paper.

DOI: 10.1021/acsami.9b15180
ACS Appl. Mater. Interfaces 2020, 12, 2601−2606

Notes

The authors declare no competing financial interest.

■ ACKNOWLEDGMENTS

This work was supported by the National Natural Science Foundation of China (21404015, 61774155, NSFC, 61705227, 91750205), National Key Research and Development Program of China (2018YFB1107202, 2017YFB1104700),and Jilin Technology and Science Department Project (20180414019GH, 20150204019GX).

■ REFERENCES

(1) Krishnan, Y.; Simmel, F. C. Nucleic Acid Based Molecular Devices. *Angew. Chem., Int. Ed.* **2011**, *50*, 3124−3156.
(2) DelRosso, N. V.; Hews, S.; Spector, L.; Derr, N. D. A Molecular Circuit Regenerator to Implement Iterative Strand Displacement Operations. *Angew. Chem., Int. Ed.* **2017**, *56*, 4443−4446.
(3) de Silva, P. A.; Gunaratne, N. H. Q.; McCoy, C. P. A Molecular pPhotoionic AND Gate Based on Fluorescent Signaling. *Nature* **1993**, *364*, 42−44.
(4) Zhou, C.; Liu, D.; Wu, C.; Liu, Y.; Wang, E. Integration of DNA and Graphene Oxide for the Construction of various Logic Circuits. *Nanoscale* **2016**, *8*, 17524−17531.
(5) Zhou, C.; Liu, D.; Dong, S. Innovative Bimolecular-Based Advanced Logic Operations: A Prime Discriminator and An Odd Parity Checker. *ACS Appl. Mater. Interfaces* **2016**, *8*, 20849−20855.
(6) Benenson, Y.; Gil, B.; Ben-Dor, U.; Adar, R.; Shapiro, E. An Autonomous Molecular Computer for Logical Control of Gene Expression. *Nature* **2004**, *429*, 423−429.
(7) Zhou, C.; Liu, D.; Wu, C.; Dong, S.; Wang, E. Multifunctional Graphene/DNA-Based Platform for the Construction of Enzyme-Free Ternary Logic Gates. *ACS Appl. Mater. Interfaces* **2016**, *8*, 30287−30293.
(8) Elbaz, J.; Lioubashevski, O.; Wang, F.; Remacle, F.; Levine, R. D.; Willner, I. DNA Computing Circuits Using Libraries of DNAzyme Subunits. *Nat. Nanotechnol.* **2010**, *5*, 417−422.
(9) Qian, L.; Winfree, E.; Bruck, J. Neural Network Computation with DNA Strand Displacement Cascades. *Nature* **2011**, *475*, 368−372.
(10) Zhang, D. Y.; Winfree, E. Control of DNA Strand Displacement Kinetics Using Toehold Exchange. *J. Am. Chem. Soc.* **2009**, *131*, 17303−17314.
(11) Qian, L.; Winfree, E. Scaling Up Digital Circuit Computation with DNA Strand Displacement Cascades. *Science* **2011**, *332*, 1196−1201.
(12) Chao, J.; Wang, J.; Wang, F.; Ouyang, X.; Kopperger, E.; Liu, H.; Li, Q.; Shi, J.; Wang, L.; Hu, J.; Wang, L.; Huang, W.; Simmel, F. C.; Fan, C. Solving Mazes with Single-molecule DNA Navigators. *Nat. Mater.* **2019**, *18*, 273−279.
(13) Willner, I.; Shlyahovsky, B.; Zayats, M.; Willner, B. DNAzymes for Sensing, Nanobiotechnology and Logic Gate Applications. *Chem. Soc. Rev.* **2008**, *37*, 1153−1165.
(14) Mailloux, S.; Gerasimova, Y. V.; Guz, N.; Kolpashchikov, D. M.; Katz, E. Bridging the Two Worlds: A Universal Interface between Enzymatic and DNA Computing Systems. *Angew. Chem., Int. Ed.* **2015**, *54*, 6562−6566.
(15) Zhou, C.; Geng, H.; Guo, C. Design of DNA-based innovative computing system of digital comparison. *Acta Biomater.* **2018**, *80*, 58−65.
(16) Zhou, C.; Wang, K.; Fan, D.; Wu, C.; Liu, D.; Liu, Y.; Wang, E. An Enzyme-free and DNA-based Feynman Gate for Logically Reversible Operation. *Chem. Commun.* **2015**, *51*, 10284−10286.
(17) Prokup, A.; Deiters, A. Interfacing Synthetic DNA Logic Operations with Protein Outputs. *Angew. Chem., Int. Ed.* **2014**, *53*, 13192−13195.
(18) Feng, L.; Lyu, Z.; Offenhäusser, A.; Mayer, D. Multi-level Logic Gate Operation Based on Amplified Aptasensor Performance. *Angew. Chem., Int. Ed.* **2015**, *54*, 7693−7697.
(19) Adleman, L. Molecular Computation of Solutions to Combinatorial Problems. *Science* **1994**, *266*, 1021−1024.
(20) Bi, S.; Chen, M.; Jia, X.; Dong, Y.; Wang, Z. Hyperbranched Hybridization Chain Reaction for Triggered Signal Amplification and Concatenated Logic Circuits. *Angew. Chem., Int. Ed.* **2015**, *54*, 8144−8148.
(21) Wang, W.; Huang, S.; Li, J.; Rui, K.; Bi, S.; Zhang, J.-R.; Zhu, J.-J. Evaluation of Intracellular Telomerase Activity Through Cascade DNA Logic Gates. *Chem. Sci.* **2017**, *8*, 174−180.
(22) Zhang, C.; Yang, J.; Jiang, S.; Liu, Y.; Yan, H. DNAzyme-Based Logic Gate-Mediated DNA Self-Assembly. *Nano Lett.* **2016**, *16*, 736−741.
(23) You, M.; Zhu, G.; Chen, T.; Donovan, M. J.; Tan, W. Programmable and Multi-parameter DNA-Based Logic Platform for Cancer Recognition and Targeted Therapy. *J. Am. Chem. Soc.* **2015**, *137*, 667−674.
(24) Mailloux, S.; Gerasimova, Y. V.; Guz, N.; Kolpashchikov, D. M.; Katz, E. Bridging the Two Worlds: A Universal Interface between Enzymatic and DNA Computing Systems. *Angew. Chem., Int. Ed.* **2015**, *54*, 6562−6566.
(25) Guo, Y.; Wu, J.; Ju, H. Target-driven DNA Association to Initiate Cyclic Assembly of Hairpins for Biosensing and Logic Gate Operation. *Chem. Sci.* **2015**, *6*, 4318−4323.
(26) Chen, J.; Fang, Z.; Lie, P.; Zeng, L. Computational Lateral Flow Biosensor for Proteins and Small Molecules: A New Class of Strip Logic Gates. *Anal. Chem.* **2012**, *84*, 6321−6325.
(27) Zhu, J.; Wang, L.; Xu, X.; Wei, H.; Jiang, W. Modular Nuclease-Responsive DNA Three-Way Junction-Based Dynamic Assembly of a DNA Device and Its Sensing Application. *Anal. Chem.* **2016**, *88*, 3817−3825.
(28) Ge, L.; Wang, W.; Sun, X.; Hou, T.; Li, F. Versatile and Programmable DNA Logic Gates on Universal and Label-Free Homogeneous Electrochemical Platform. *Anal. Chem.* **2016**, *88*, 9691−9698.
(29) Chen, J.; Pan, J.; Chen, S. A Label-free and Enzyme-free Platform with a Visible Output for Constructing Versatile Logic Gates using Caged G-quadruplex as the Signal Transducer. *Chem. Sci.* **2018**, *9*, 300−306.
(30) Krishnan, Y.; Simmel, F. C. Nucleic Acid Based Molecular Devices. *Angew. Chem., Int. Ed.* **2011**, *50*, 3124−3156.
(31) Wang, F.; Liu, X.; Willner, I. DNA Switches: From Principles to Applications. *Angew. Chem., Int. Ed.* **2015**, *54*, 1098−1129.
(32) Tang, Y.; Ge, B.; Sen, D.; Yu, H.-Z. Functional DNA Switches: Rational Design and Electrochemical Signaling. *Chem. Soc. Rev.* **2014**, *43*, 518−529.
(33) Zhou, C.; Geng, H.; Wang, P.; Guo, C. Programmable DNA Nanoindicator-Based Platform for Large-Scale Square Root Logic Biocomputing. *Small* **2019**, *15*, 1903489.
(34) Geng, H.; Zhou, C.; Guo, C. DNA-based digital comparator systems constructed by multifunctional nanoswitches. *Nanoscale* **2019**, *11*, 21856−21866.

DOI: 10.1021/acsami.9b15180
ACS Appl. Mater. Interfaces 2020, 12, 2601−2606